International Journal of Fluid Machinery and Systems
Vol. 3, No. 3, July-September 2010

DOI: 10.5293/IJFMS.2010.3.3.227
ISSN (Online): 1882-9554

Original Paper

Numerical Study on Mixing Performance of Straight Groove Micromixers

Shakhawat Hossain and Kwang-Yong Kim

Department of Mechanical Engineering, Inha University
253 Yonghyun-Dong, Incheon, 402-751, Republic of Korea
shakhawat@inha.edu, kykim@inha.ac.kr

Abstract

Numerical analyses have been performed to investigate the effects of geometric parameters of a straight groove micromixer on mixing performance and pressure drop. Three-dimensional Navier-Stokes equations with two working fluids, water and ethanol have been used to calculate mixing index and pressure drop. A parametric study has been carried out to find the effects of the number of grooves per cycle, arrangement of patterned walls, and additional grooves in triangular dead zones between half cycles of grooves. The three arrangements of patterned walls in a micromixer, i.e., single wall patterned, both walls patterned symmetrically, and both walls patterned asymmetrically, have been tested. The results indicate that as the number of grooves per cycle increases the mixing index increases and the pressure drop decreases. The microchannel with both walls patterned asymmetrically shows the best mixing performance among the three different arrangements of patterned walls. Additional grooves confirm the better mixing performance and lower pressure drop.

Keywords: Micromixer; Straight Groove; Numerical Analysis; Mixing; Navier-Stokes Equations, Pressure Drop

1. Introduction

With the help of microtechnology applied to microfluidics, miniaturized chemical and biological analysis units offer a wide range of opportunities in terms of applications and performances. In recent years the micromixer has emerged as a fundamental component for the realization of micro total analysis systems (μTAS) or lab-on-a-Chip. Due to the small scale, flows in micromixers are laminar flows associated with a very low Reynolds number (<1). The dimension of a microfluidic device is typically sub-millimeter and conventional methods to stir the fluids are not applicable, so it is very difficult to mix the fluids at a microscopic scale. In laminar flows, the mixing solely depends on the molecular diffusion, which is usually a very slow process. So in many applications, it is necessary to apply specially designed geometries to micromixers to enhance mixing [1,2]. In the case of two fluids flowing in a channel side by side, a well defined interface appears and only diffusion creates mixing. Increasing the mixing rate is an important issue for many microfluidic applications.

In order to enhance fluid mixing in microchannels, various types of active and passive micromixers have been developed. Active micromixers depend on an external source of energy to force fluids to mix together inside the microchannel [3]. Active micromixers generally improve mixing by stirring the flow in order to create secondary flows. This stirring effect can be achieved by using additional structures or external sources including acoustic wave, electrokinetic field, or magnetic field techniques. Passive micromixers do not require external energy; the mixing process relies entirely on diffusion or chaotic advection. Passive mixers can be further categorized as lamination micromixers and injection micromixers. In lamination mixers, the fluid streams are split into several small streams, which are later joined in a mixing channel [2]. In contrast to lamination mixers, an injection mixer splits only one stream into many substreams in the form of microplumes, which increase the contact surface and decrease the mixing path. Active micromixers are generally more complex and can thus be difficult to operate, fabricate, clean, and integrate into microfluidic systems. Therefore, passive mixers are used in most microfluidic applications.

Many researchers have designed passive micromixers with various mechanisms. Experimentally, Stroock et al. [4] studied mixing performance in a passive micromixer by placing straight grooves on the floor in a rectangular microchannel, where secondary flows are formed on cross-sectional planes and the flow streamlines in the channel become helical. Similar transversal flows were also observed by Johnson et al. [5]. To evaluate the effects of chaotic advection, patterned groove microchannels were numerically investigated by Wang et al. [6]. They reported that micromixers with patterned grooves cause rotation of the fluid streams, which can reorient the

Received August 10 2010; accepted for publication August 24 2010: Review conducted by Dr. Shogo Nakamura. (Paper number O10021J)
Corresponding author: Kwang-Yong Kim, Professor, kykim@inha.ac.kr

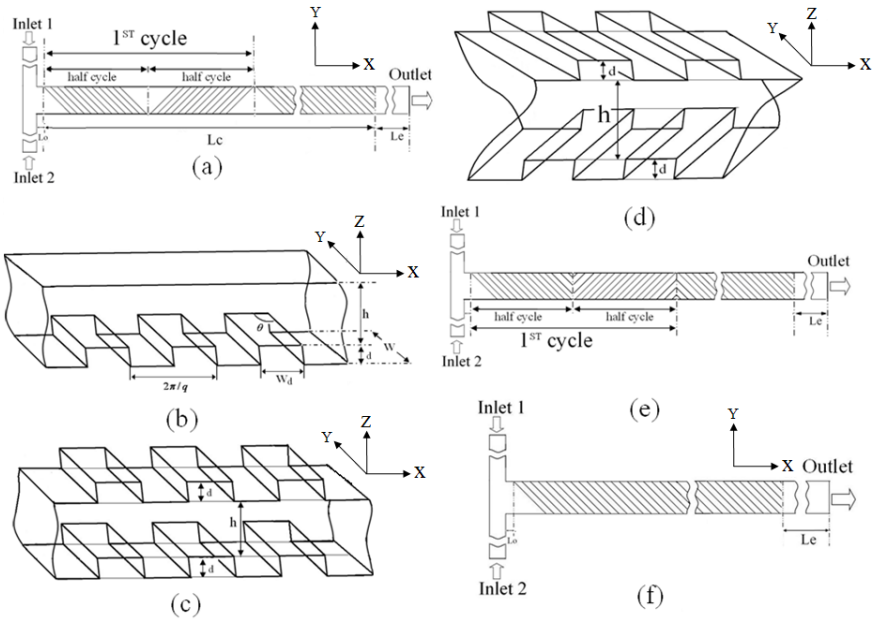

Fig. 1 Schematic diagrams of micromixer geometries: (a) patterned groove micromixer, (b) single wall patterned, (c) both wall patterned symmetrically, (d) both wall patterned asymmetrically, (e) patterned groove micromixer with additional grooves in dead zones, and (f) base geometry micromixer.

folding in the depth direction, and can improve passive mixing performance. Schönfeld and Hardt [7] investigated helical flows in structured microchannels by using a CFD method, and proposed a new type of micromixer with grooves on top and bottom which can produce the transition of the secondary flow pattern from two to four vortices. By performing a computational analysis of mixing, Lin [8] reported that a new micromixer composed of a lengthways channel with patterned grooves on the bottom and side of the channel shows a better performance than the well-known staggered herringbone micromixer.

As mentioned above, a variety of experimental and numerical studies on mixing have been carried out with patterned groove micromixers. In this study, a parametric study on micromixers with patterned grooves has been performed by solving three-dimensional Navier-Stokes equations. Water and ethanol have been selected as the two working fluids for mixing. The purpose of the present work is to test the effects of the number of grooves per cycle on mixing in a micromixer patterned with straight grooves, to analyze the mixing performances and flow structure in three different patterned groove micromixers, and to examine the effects of additional grooves on mixing. Mixing index and pressure drop have been considered as the performance parameters.

2. Numerical Formulation

Fig. 1 demonstrates the schematic diagrams of the straight groove micromixers tested in the present work. Two different fluids enter from two inlets, as shown in Fig. 1(a), and there is an outlet on the right side. The two inlets, Inlet 1 and Inlet 2, merge in the main microchannel with a T-joint. Water and ethanol are used as the two operating fluids for mixing (Table 1). Fig. 1(b) represents the main unit of the straight groove microchannel, The dimensions are as follows: channel width, w = 0.2 mm; groove width, w_d = 0.05 mm; channel height, h = 0.077 mm; depth of the groove, d = 0.01771 mm; angle of the groove, $\theta = 45^o$; and groove pitch length, $2\pi/q$ = 0.1 mm. Figs. 1(c) and 1(d) show the straight groove microchannels with both (bottom and top) walls roughened by the grooves in same and opposite directions, respectively. Fig. 1(a) shows the straight groove channel with the number of grooves per cycle being 14. To investigate the effects of the number of grooves per cycle on mixing, the straight groove micromixers with the number of grooves per cycle being 8, 14, and 20, respectively, have been tested. Due to a periodic change of direction of grooves per half cycle, triangular dead zones between half cycles are induced. To remove these dead zones, additional grooves are introduced as shown in Fig. 1(e), and the effects have been tested. The total length of the channel is fixed at 7.5 mm, which is the sum of the channel section lengths, i.e., Lo, Lc, and Le.

A commercial CFD-code, ANSYS CFX-11.0 [9], has been used to analyze the flow and mixing in the micromixers. This is a general purpose code that solves Navier–Stokes equations using the finite volume method via a coupled solver. The steady three-dimensional continuity and momentum (Navier–Stokes) equations are solved in this work.

To analyze the actual mixing phenomena, Navier-Stokes equations in combination with an advection-diffusion model are solved. An unstructured tetrahedral grid system is created by ANSYS ICEM 11.0. Grid-dependency test has been carried out in preliminary stage of this work, and the grids selected in this test have been used in main calculations.

Table 1 Reference and optimal shape

Fluid	Density(kg m^{-3})	Viscosity (Kg m^{-1} s^{-1})	Diffusivity (m^2 s^{-1})
Water	9.998×10^2	0.9×10^{-3}	1.2×10^{-9}
Ethanol	7.890×10^2	1.2×10^{-3}	1.2×10^{-9}

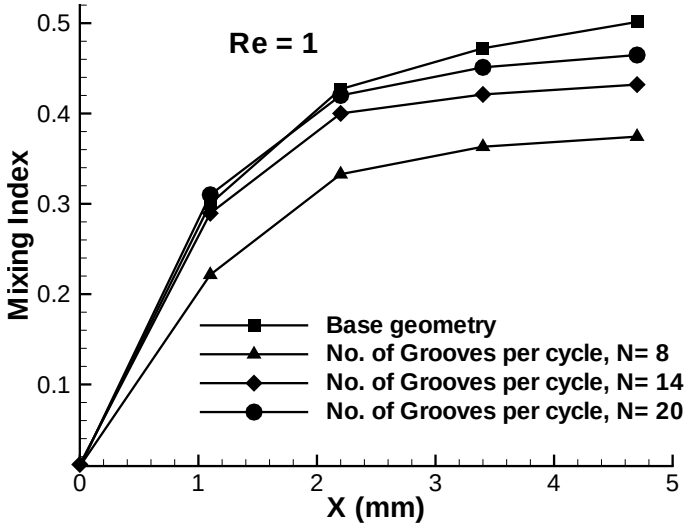

Fig. 2 Mixing index distributions with different numbers of grooves per cycle

The numerical simulation is not free from numerical diffusion errors, which arise from the discretization of the convection terms in the Navier-Stokes equations. Numerical diffusion cannot be completely ignored; however, it can be minimized by adopting certain techniques [10]. The velocity at the inlets and zero static pressure at the outlet are specified as the boundary conditions. The solutions are considered to have attained convergence when the value of the root-mean-squared (rms) relative residual is at most 10^{-6}.

To quantify and analyze mixing, the variance of the fluid species in the micromixer has been calculated. The variance of species is determined in a cross-sectional area of the micromixer perpendicular to the x-axis. The variance is based on the concept of the intensity of segregation, which is based on the variance of the concentration with the mean concentration. To evaluate the degree of mixing in the micromixer, the variance of the mass fraction of the mixture in a cross-section that is normal to the flow direction is defined as follows.

$$\sigma = \sqrt{\frac{1}{N}\sum (c_i - \bar{c}_m)^2} \tag{1}$$

In the above definition, N is the number of sampling points inside the cross-section, c_i is the mass-fraction at sampling point i, and c_m is the optimal mixing mass fraction. To quantitatively analyze the mixing performance of the micromixer, the mixing index is defined as follows.

$$M = 1 - \sqrt{\frac{\sigma^2}{\sigma^2_{\max}}} \tag{2}$$

where, σ is the standard deviation of the concentration across the channel in a cross-section at any specific longitudinal location, and $\sigma_{\max}$ is the maximum standard deviation (unmixed at the exit). A greater mixing index indicates a higher mixing quality: the value of this mixing index is thus zero for completely separate streams (for which $\sigma = \sigma_{\max}$), and unity for completely mixed streams (for which $\sigma = 0$). For all geometries, the mixing index has been calculated after a single unit for comparing the results across geometries.

3. Results and Discussion

3.1 Effects of the number of grooves per cycle

To investigate the effects of the number of grooves per cycle on mixing, the straight groove micromixers with the number of grooves per cycle being 8, 14, and 20, respectively, have been tested for the geometry shown in Fig. 1(a) and Fig. 1(b). Fig. 2 represents the mixing index distributions in the micromixers with different numbers of grooves per cycle. The base geometry shown in Fig. 1(f) indicates a micromixer without periodic change of direction of grooves. Mixing indexes are plotted along the channel length (x-direction) at Reynolds number 1. The distributions represent that with an increase in the number of grooves per cycle the mixing index increases, and the base geometry shows the best mixing performance. Mixing indexes have been calculated for equal axial length in every case. For a fixed axial length, the number of cycles (i.e., number of triangular dead zones) decreases with an increase in the number of grooves per cycle. It means that the disturbances caused by the triangular dead zones and/or the changes of groove direction do not contribute to the enhancement of mixing performance at all. Therefore, the best mixing performance occurs at the base geometry.

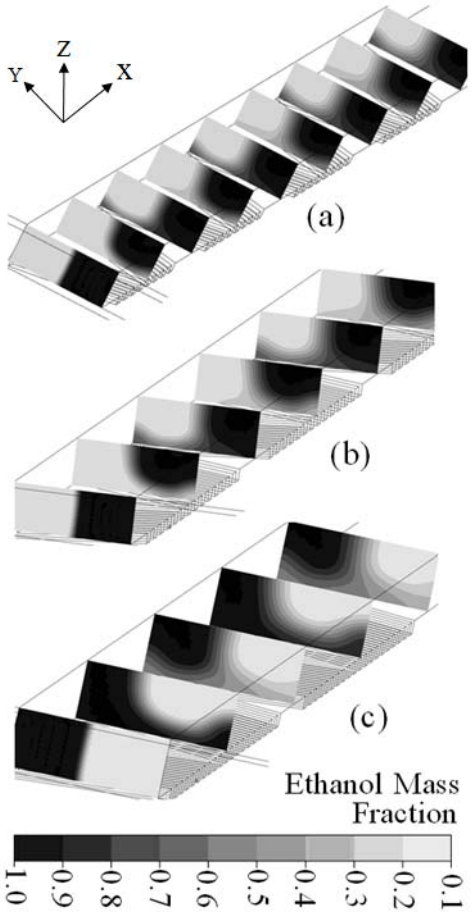

Fig. 3 Mass fraction distributions of ethanol for different numbers of grooves per cycle: (a) 8, (b) 14, and (c) 20.

Fig. 3 demonstrates the mass fraction distributions of ethanol for different numbers of grooves per cycle. The mass fraction distributions of ethanol have been plotted on a yz-plane perpendicular to the main flow direction for Re = 1. Fig. 3(a), (b), and (c) represent the distributions with the number of grooves per cycle being 8, 14, and 20, respectively. Concentration distribution has been plotted after each half cycle. The figure visualizes a similar pattern of concentration distribution of ethanol at the first plane. Fig. 3(c) represents similar concentration distribution pattern at alternate planes and also visualizes two identical half vortices over the cross sectional plane. Due to the alternate change of direction of the grooves, the concentration structure changes per half-cycle. Fig. 3(a) and 3(b) characterize the change of interface of fluids per half cycle, which indicates the change of flow direction in the same pattern.

Table 2 illustrates the comparison of pressure drops with different numbers of grooves per cycle. Pressure drop is directly related to the energy input used for the mixing process. The pressure drops are calculated between the two planes; the plane at the main channel inlet and the plane at the outlet. Equal axial length has been considered for the pressure drop calculations. The results explain that the straight groove geometry with the number of grooves per cycle being 8 shows the highest pressure drop, and that with the increase of the number of grooves per cycle, the pressure drop decreases. Increased number of the changes of flow direction per half cycle increases the pressure drop. Thus, the base geometry shows the lowest pressure drop.

3.2 Effects of different arrangements of patterned walls

To evaluate the mixing performance in different arrangements of the patterned walls in a straight groove micromixer, three different arrangements, namely straight grooves patterned on the bottom wall, symmetrically patterned on both walls, and

Table 2 Pressure drops with different numbers of grooves per cycle

No. of grooves per cycle	Pressure drop (Pa)
N=8	267.0
N=14	252.1
N=20	243.4
Base geometry	239.8

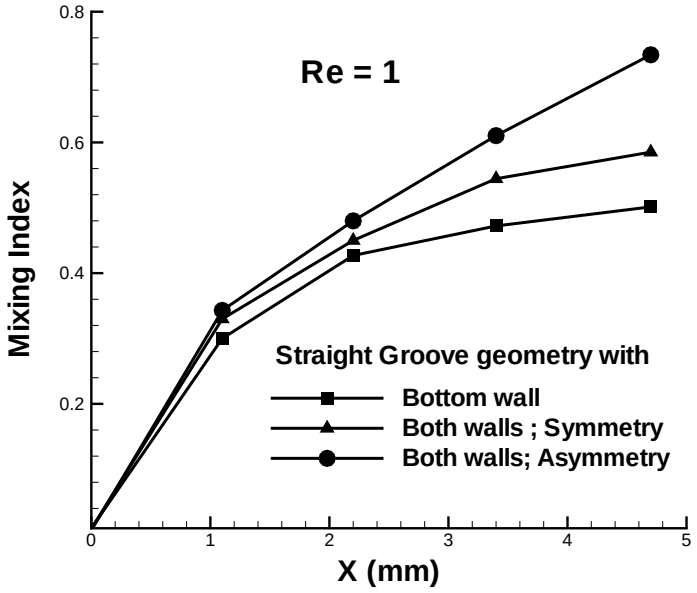

Fig. 4 Mixing index distributions for different arrangements of patterned walls.

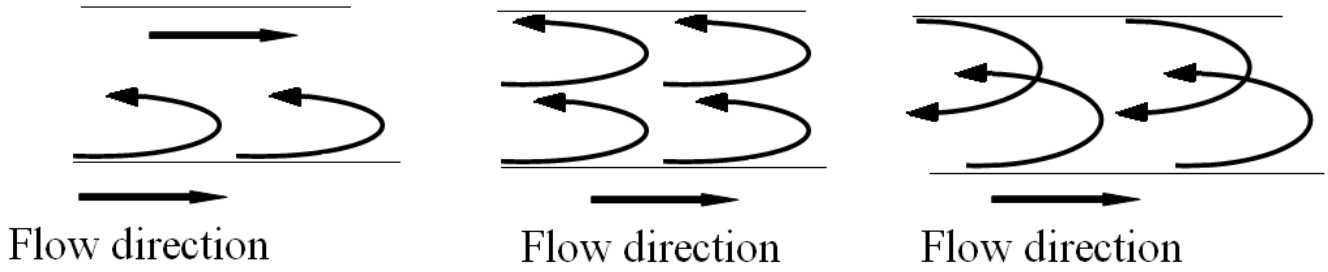

(a) single wall patterned (b) both walls patterned symmetrically (c) both walls patterned asymmetrically.

Fig. 5 Flow structure of arrangements of patterned walls:

asymmetrically patterned on both walls, have been considered. Fig. 4 shows the mixing index distributions in the different arrangements of patterned walls. Mixing indexes are plotted along the channel length (in the x-direction) at Reynolds number 1. The mixing index in the straight groove microchannel with asymmetrically patterned grooves on both walls has a value 1.47 times larger than that in the base microchannel (only bottom wall patterned with grooves) and 1.25 times larger than that in the microchannel with symmetrically patterned walls at the end of the grooves. In the case of the asymmetric geometry, due to the staggered arrangement of the grooves, the fluids near the bottom and top walls are disturbed in opposite directions which enhance the mixing performance.

Two-dimensional flow structures are illustrated in Fig. 5 for the three different patterned groove micromixers. Fig. 5(a) visualizes counterclockwise rotation of the flow near the bottom wall due to the diagonal grooves, but the flow near the top wall is not affected by the grooves and is parallel to the wall. In the case of the symmetric geometry, Fig. 5(b) shows both flows near the bottom and top walls rotate counterclockwise. However, in the asymmetric case, Fig. 5(c) demonstrates the flow near the bottom wall rotates counterclockwise while the flow near the top wall rotates in the opposite direction, and at the middle of the channel height the flows collide, which enhances the mixing performance. Fig. 6 reveals mass fraction distributions of ethanol for different straight groove geometries. The mass fraction distributions of ethanol has been plotted on a yz-plane perpendicular to the main flow direction for Re = 1. Fig. 7 shows that the fluid near the walls is transported in the direction of walls. In case of both walls patterned asymmetrically shown in Fig. 6(c), the opposite directions of the fluids near the walls cause a strong vortex at the center and the mixing is enhanced.

Fig. 7(a) to 7(c) illustrate the velocity vector plots on a yz-plane perpendicular to the main flow direction for the three different arrangements at Reynolds number 1. These figures visualize induced secondary vortices over the cross-sectional planes. Fig. 7(a) shows induced vortices near the bottom wall, while Fig. 7(b) and 7 (c) show induced vortices near the bottom and top walls. In the case of symmetric grooves, the formation of vortices is also symmetric as shown in Fig. 7(b). On the other hand, in the case of asymmetric grooves, the vortical structure is also asymmetric, and the interactions between upper and lower vortices become more complex. Table 3 illustrates the comparison of pressure drop among the three different arrangements of straight groove walls. Pressure drop is directly related to the energy input used for the mixing process. Axial length of the microchannels has been fixed for the comparison. The micromixer with a single wall pattern shows the lowest pressure drop and the micromixer with an asymmetric geometry shows the highest pressure drop due to the staggered groove arrangement.

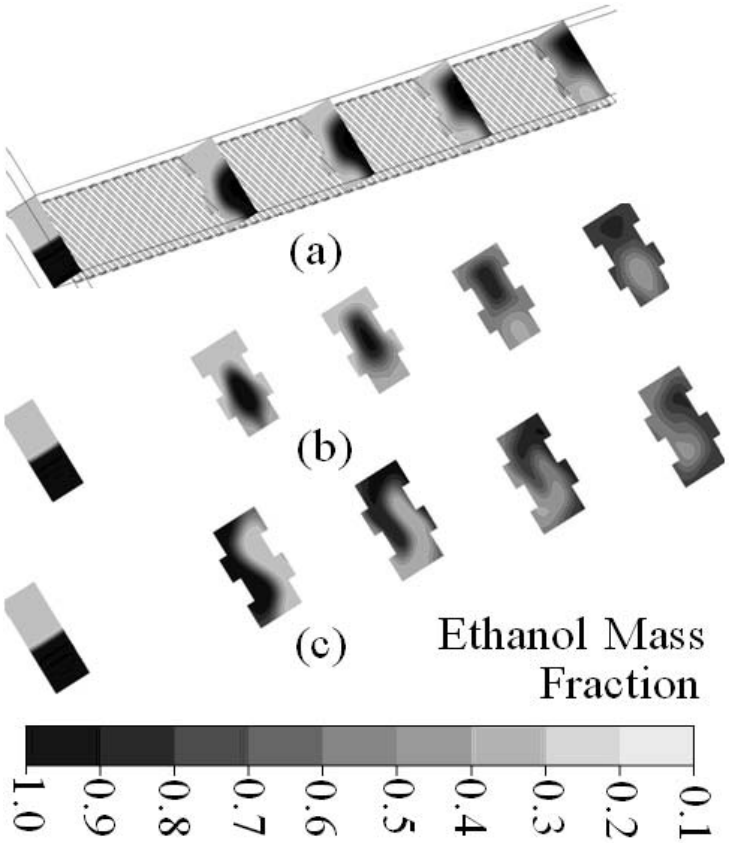

Fig. 6 Mass fraction distributions of ethanol for different arrangements of patterned walls: (a) single wall patterned, (b) both walls patterned symmetrically, and (c) both walls patterned asymmetrically.

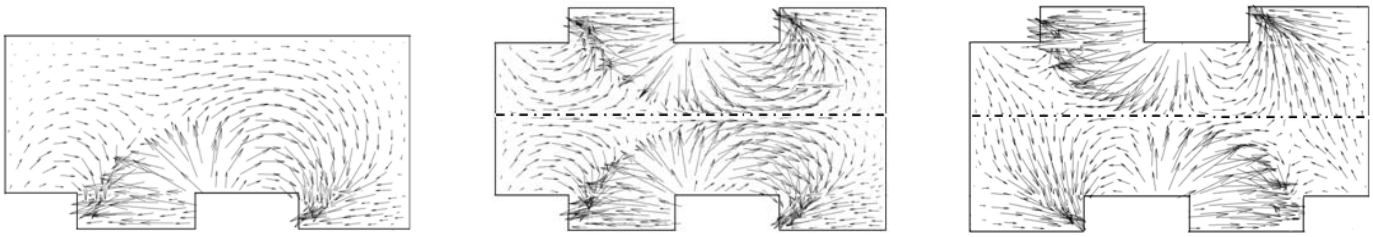

(a) single wall patterned (b) both walls patterned symmetrically (c) both walls patterned asymmetrically.

Fig. 7 Velocity vectors for different arrangements of patterned walls:

3.3 Effect of additional grooves on mixing

Effects of the additional grooves shown in Fig. 1(e) with a single wall roughened on mixing are also investigated. Fig. 8 shows the mixing index distributions in the straight groove microchannels with and without additional grooves with the number of grooves per cycle being 8. The mixing index with additional grooves is higher than that without additional grooves. This concept is also expected to be used for the staggered herringbone groove geometry to improve the mixing index. Table 4 shows that the pressure drop with additional grooves is lower than that without additional grooves. Thus, the introduction of additional grooves in the triangular dead zones between half cycles of grooves (Fig. 1(e)) reduces the pressure drop as well as improves mixing performance.

Table 3 Pressure drops with different arrangements of patterned walls.

Straight groove micromixers with	Pressure drop (Pa)
Bottom wall	239.8
Both walls, symmetry	286.1
Both walls, asymmetry	295.4

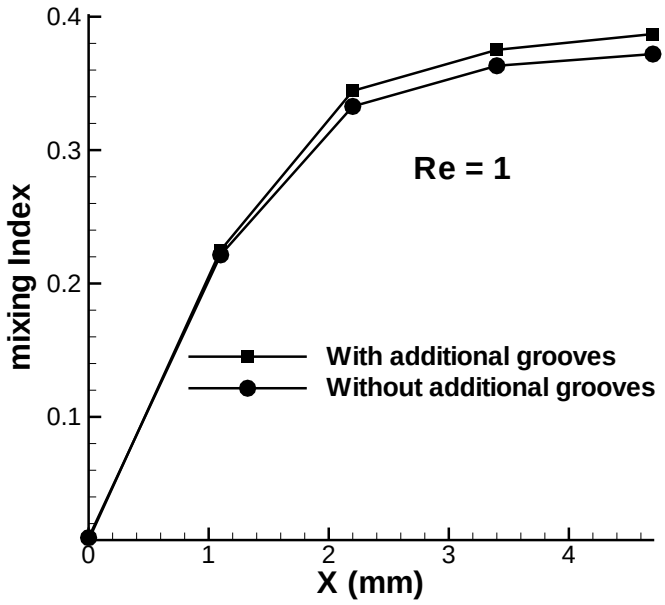

Fig. 8 Mixing index distributions with and without additional grooves (number of grooves per cycle = 8).

Table 4 Pressure drops with and without additional grooves (number of grooves per cycle = 8).

	Pressure drop (Pa)
With additional grooves	253.2
Without additional grooves	267.0

4. Conclusion

Mixing and pressure drop characteristics have been investigated with some geometric parameters in patterned microchannels with straight grooves at Reynolds number 1. Three-dimensional Navier-Stokes analyses have been performed for the analysis of flow and mixing of two fluids. The results show that the mixing performance improves and the pressure drop decreases with an increase of the number of grooves per cycle (ranging from 8 to 20) with a fixed channel length. This indicates that the change of flow direction per half cycle increases the pressure drop. The mixing index in the microchannel with asymmetrically patterned grooves on both walls has a value 1.47 times larger than that in the base microchannel with only a bottom wall patterned with grooves and 1.25 times larger than that in the microchannel with symmetrically patterned walls at the end of the grooves. Effects of additional grooves in the triangular dead zones between half cycles of grooves have also been examined. The introduction of additional grooves confirms better mixing performance as well as lower pressure drop. This concept is expected to be applied to the design of staggered herringbone grooves in order to improve mixing performance.

Acknowledgments

This research was supported by the National Research Foundation of Korea (NRF) grant No. 20090083510 funded by government (MEST) through Multi-phenomena CFD Engineering Research Center.

Nomenclature

h	Channel height	M	Mixing index
L	Channel length	R	Radius of curvature
w	Channel width	μ	Absolute viscosity of fluid, Kg $m^{-1}s^{-1}$
wd	Width of groove	ρ	Fluid density, Kg m^{-3}
d	Depth of groove	σ	Variance
N	Number of sampling points	α	Scalar diffusivity
Re	Reynolds number		

References

[1] Reyes, D. R., Iossifidis, D., Auroux, P. A., and Manz, A., 2002, "Micro Total Analysis Systems (1. Introduction, theory and technology)," Analytical Chemistry, Vol. 74, pp. 2623-2636.
[2] Nguyen, N. T. and Wu, Z., 2005, "Micromixers - review," Journal of Micromechanics and Microengineering, Vol. 15, pp. 1-16.

[3] Hessel, V., Löwe, H., and Schönfeld, F., 2005, “Micromixers - a review on passive and active mixing principles,” Chemical Engineering Science, Vol. 60, pp. 2479 - 2501.
[4] Stroock, A. D., Dertinger, S. K. W., Ajdarim, A., Mezic, I., Stone, H. A., and Whitesides, G. M., 2002, “Chaotic Mixer for Microchannels,” Science, Vol. 295, pp. 647-651.
[5] Johnson, T. J., Ross, D., and Locascio, L.E., 2002, “Rapid Microfluidic Mixing,” Analytical Chemistry, Vol. 74, pp. 45-51.
[6] Wang, H., Iovenitti, P., Harvey, E. and Masood, S., 2003, “Numerical investigation of mixing in microchannels with patterned grooves,” Journal of Micromechanics and Microengineering, Vol. 13, pp. 801-808.
[7] Schonfeld, F. and Hardt, S., 2004, “Simulation of helical flows in microchannels,” AIChE Journal, Vol. 50, pp. 771-778.
[8] Lin, W., 2008, “A Passive Grooved Micromixer Generating Enhanced Transverse Rotations for Microfluids,” Chemical Engineering & Technology, Vol. 31, pp. 1210-1215.
[9] CFX- 11.0, Solver Theory, ANSYS, 2007.
[10] Hardt, S. and Schonfeld, F., 2003, “Laminar mixing in different interdigital micromixers: II. Numerica Simulations,” AIChE Journal, Vol. 49, pp. 578-584.